

# The Formation and Structure of Olympic Gels

J. Fischer\* and M. Lang<sup>†</sup>

*Leibniz Institut für Polymerforschung Dresden,  
Hohe Straße 6, 01069 Dresden, Germany.*

J.-U. Sommer

*Leibniz Institut für Polymerforschung Dresden,  
Hohe Straße 6, 01069 Dresden, Germany. and  
Technische Universität Dresden, Institute of Theoretical Physics,  
Zellescher Weg 17, D-01069 Dresden, Germany.*

Different methods for creating Olympic gels are analyzed using computer simulations. First ideal reference samples are obtained from freely interpenetrating semi-dilute solutions and melts of cyclic polymers. The distribution of pairwise concatenations per cyclic molecule is given by a Poisson-distribution and can be used to describe the elastic structure of the gels. Several batches of linear chains decorated with different selectively binding groups at their ends are mixed in the “DNA Origami” technique and network formation is realized. While the formation of cyclic molecules follows mean field predictions below overlap of the precursor molecules, an enhanced ring formation above overlap is found that is not explained by mean field arguments. The “progressive construction” method allows to create Olympic gels with a single reaction step from a concentrated mixture of large compressed rings with a low weight fraction short chains that are below overlap concentration. This method, however, is limited by the difficulty to obtain a sufficiently high degree of polymerization of the large rings.

---

\* Present address: Bio Systems Analysis Group, Jena Centre for Bioinformatics (JCB) and Department for Mathematics and Computer Sciences, Friedrich Schiller University of Jena, 07743 Jena, Germany.

<sup>†</sup> lang@ipfdd.de

## I. INTRODUCTION

“Olympic gels” (OGs) [1] are networks made of cyclic polymers (also called polymer rings) that are not linked by chemical cross-links. Instead, the permanent entanglement between concatenated rings establishes a three dimensional network structure similar to the structure of the Olympic rings. Due to the lack of cross-links, these samples were considered to be ideal model networks that might allow for an unperturbed analysis of the effect of entanglements in a polymer network [2]. Recently [3], it was shown by computer simulations that OGs show unusual swelling properties, since networks of longer strands swell less than networks made of short cyclic molecules at otherwise identical preparation conditions. This was explained [3] by the desinterspersion of overlapping non-concatenated rings, that causes a large non-affine contributions to the swelling of these gels at the available low average number of concatenations per ring.

Even though these OGs are, therefore, a very interesting model system to understand the physics of entanglements, these network have not yet been synthesized. The reason for this can be understood from considering the geometry of cyclization: Let us consider a mono-disperse solution of linear  $N$ -mers that are long enough for cyclization. In order to form an OG, the cyclic molecules have to be at sufficient overlap such that a sufficiently large average number of concatenations per ring,  $f_n$ , can be established. Let  $P \approx \phi R^3/(Nv_0)$  denote the number of overlapping linear chains of the same degree of polymerization  $N$ , monomeric unit volume  $v_0$  and size  $R$  at a polymer volume fraction of  $\phi$ . Gel formation, therefore, requires  $P \gg 1$  and a weight average of at least two connections per molecule. However, the probability that the  $N$ -mer forms a ring is only of order  $\approx 1/(2P)$ , since there is only one opposite end of the same chain to react with in the pervaded volume. Therefore, even if all  $P/(2P)$  overlapping rings were mutually concatenated, these rings would not form a gel, since there is less than one connection per ring. Interestingly, this discussion depends only on  $P$  (which even cancels out) and not explicitly on  $\phi$  and  $N$ . Therefore, one cannot tune  $N$  or  $\phi$  such that an OG might be obtained. Instead, one has to modify the synthesis to allow for the formation of OG’s. In this respect, Raphael *et al.* [4] (based upon an idea of De Gennes [1]) and Pickett [5] proposed two different methods for preparing OGs as sketched in Figure 1.

The first method by De Gennes [1] is called “progressive construction”, since the network structure is built up in several steps. First, large ring polymers are made at very dilute concentrations in order to suppress the competing growth of linear chains. Next, the solution is concentrated above the overlap concentration of the rings. Then, end-functionalized linear chains are allowed to diffuse into the solution, whereby the concentration of linear chains is chosen be-

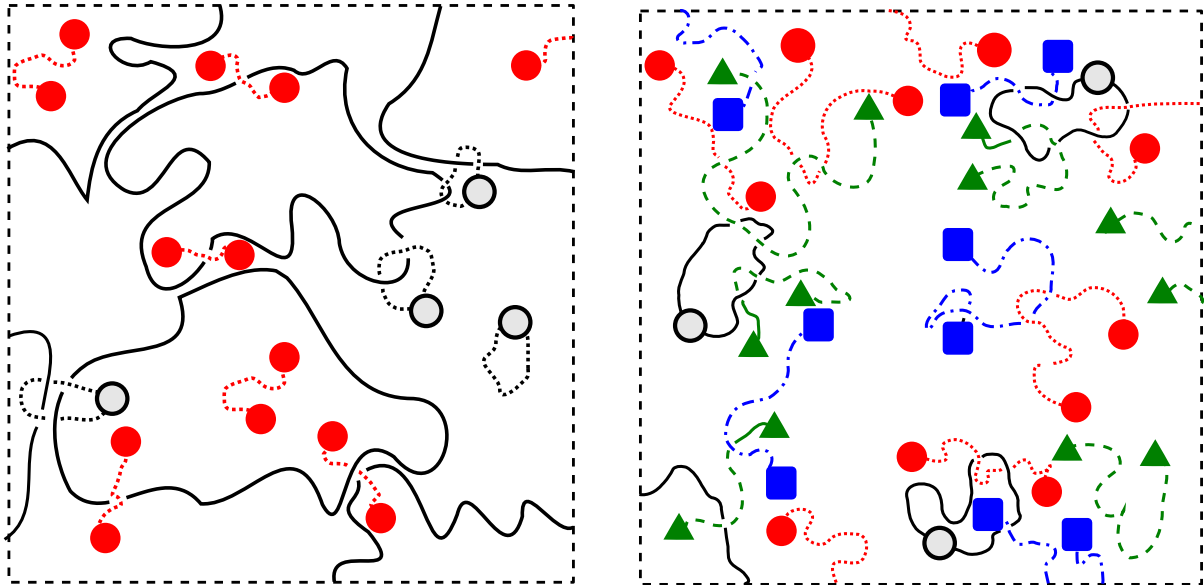


Figure 1. Progressive construction (left) and DNA-Origami (right). Lines represent polymers, dots of same color (color online all Figures) are reactive end-groups of same type and gray dots with black boundary are reacted polymer end-groups.

low the overlap concentration of the linear chains in order to promote cycle formation. When the mixing equilibrium is reached, the reaction is started and a fraction of the surrounding cyclic polymer is entrapped by the closure of the linear polymers, see left of Fig 1, which may lead to an OG, if a sufficiently large number of connections between the long rings are established.

The “DNA-Origami” approach of Pickett [5] requires the fabrication of a large set of different selectively binding end-groups. Pickett proposed to isolate a large set of different DNA fragments and to attach the ends of one chain to the two strands of one of these fragments. At solvent conditions under which DNA denaturates, the small DNA fragments will open up and the polymers decorated with the single strands of these fragments on both ends will form a linear solution of polymers. If the solvent conditions are modified such that the opposite DNA fragments stick together, the polymers can form rings upon selectively binding with the corresponding DNA fragment. If the number of different fragments is sufficiently large, OG’s are obtained because chains of same type of fragment will be below overlap concentration and thus, ring formation will dominate the growth of linear chains.

In addition to these methods, one could also use topoisomerase to create OGs of nearly perfect structure from semi-dilute solutions of cyclic DNA. We created OGs in similar manner by allowing the polymer strands to interpenetrate freely in our computer simulations. The data of these simulations is used below as ideal reference systems due to the missing polydispersity of the cyclic molecules and the absence of linear chains. In the present paper, we test these

different approaches concerning their applicability to produce OGs and concerning the quality of the network structure that can be obtained in this way both analytically and by computer simulations.

## II. COMPUTER SIMULATIONS AND ANALYSIS

We use the bond-fluctuation model (BFM) [6, 7] to simulate solutions of linear chains and rings. This method was chosen, since it is known to reproduce conformational properties and dynamics of melts [8, 9] and semi-dilute solutions [10, 11] and polymer networks [12, 13]. In this method, each monomer is represented by a cube occupying eight lattice sites on a cubic lattice. The bonds between monomers are restricted to a set of 108 bond vectors which ensure cut-avoidance of polymer strands by checking for excluded volume. Monomer motion is modeled by random jumps to one of the six nearest lattice positions. A move is accepted, if the bonds connecting to the new position are still among the set of 108 bond vectors and if no monomers overlap. All samples of the present study were created in simulation boxes with periodic boundary conditions. A-thermal solvent is treated implicitly by empty lattice sites.

In our work, we discuss two different series of simulations in order to analyze ideal OG and the competition between growth of linear chains and ring formation (DNA-Origami). The results of these simulations serve as input to analyze the “progressive construction” method. The details of sample preparation of these simulation series are summarized at the beginning of the corresponding sections.

For analysis of network connectivity, rings were first simplified at conserved topology in one additional simulation run by removing monomers  $i$  from the chain contour, whenever monomers  $i$ ,  $i+1$  and  $i-1$  formed a tight triangle through which no bond of any other molecule could pass [14]. Next, we determined a regular projection of any pair of overlapping rings with minimum number of intersections as also described in [14]. Finally, we computed the Gauss code of the projection as input for the Skein-Template algorithm of Gouesbet *et al.* [15]. The types of the knots and pairwise links formed were analyzed by using the resulting HOMFLY polynomials [16]. Data of previous work [17] show that the effect of Brunnian links or similar structures that are not (entirely) detected by a pairwise linking analysis should be ignorable for the degrees of polymerization of our study. Therefore, we restricted our connectivity analysis to pairwise links only. The resulting connectivity matrix between pairs of rings is used to analyze the network structure, weight fraction of gels, the gel point position, and the amount of the elastically active rings.

### III. IDEAL OLYMPIC GELS

Interpenetrating solutions of mono-disperse cyclic polymers are considered to serve as an ideal reference system to understand the formation of OGs, since in these samples, concatenation is in equilibrium with the polymer conformations in solution at the particular polymer concentration. Our simulations of these ideal OGs cover an array of different degrees of polymerization  $N = 16, 32, 64, 128, 192, 256, 384, 512, 768, \text{ and } 1024$  and polymer volume fractions of  $\phi = 0.5, 0.375, 0.25, 0.1875, 0.125, 0.0625, \text{ and } 0.03125$  as described previously [11]. The numbers of rings per sample varied from 512 to 4096, resulting in a simulation box size between  $128^3$  and  $512^3$  lattice sites. Periodic boundary conditions were applied in all space directions. During equilibration, additional “diagonal” moves were allowed that do preserve connectivity of a ring but allow for a change in the topology of overlapping rings, since all entanglements are switched off. After equilibration, all “x-traps” (pairs of bonds that mutually block each other’s motion - these arise here from switching off diagonal moves) [18] were removed while returning to the original set of moves and network connectivity is analyzed as described in the previous section.

In our preceding work [11], we analyzed only the average number of concatenated rings per ring polymer, the number average “functionality” of the rings,  $f_n$ , in a solution of mono-disperse interpenetrating rings in order to develop a model for the conformations of rings in melt or solution. It was found that

$$f_n \approx \gamma \phi^{\nu/(3\nu-1)} N (1 - P_{\text{OO}}), \quad (1)$$

with a numerical constant  $\gamma \approx 0.034 \pm 0.001$  and a cut-off  $(1 - P_{\text{OO}})$  for very small  $\phi^{\nu/(3\nu-1)} N$  based upon the probability for non-concatenation  $P_{\text{OO}} \approx \exp(-(\phi^{\nu/(3\nu-1)} N - a)/N_{\text{OO}})$ . Here,  $N_{\text{OO}}$  is the cross-over degree of polymerization (as defined for extrapolating to  $\phi = 1$ ) that distinguishes between the non-concatenated regime  $N < N_{\text{OO}}$  and the concatenated regime  $N > N_{\text{OO}}$ . Similar to knotting, a second parameter  $a$  is used that can be understood as effective minimum degree of polymerization to make concatenation possible (with respect to a particular environment). However, for poly-disperse systems, gelation requires [19] a *weight average* functionality  $f_w$  of two

$$f_w = 2 \quad (2)$$

instead of  $f_n = 2$ . Therefore, we have to determine  $f_w$  and the distribution of concatenations in order to estimate the position of the gel point.

In a previous work [20], it was argued that the number of concatenations per ring is related to the area of the minimal surface bounded by a ring. A rather narrow distribution of the

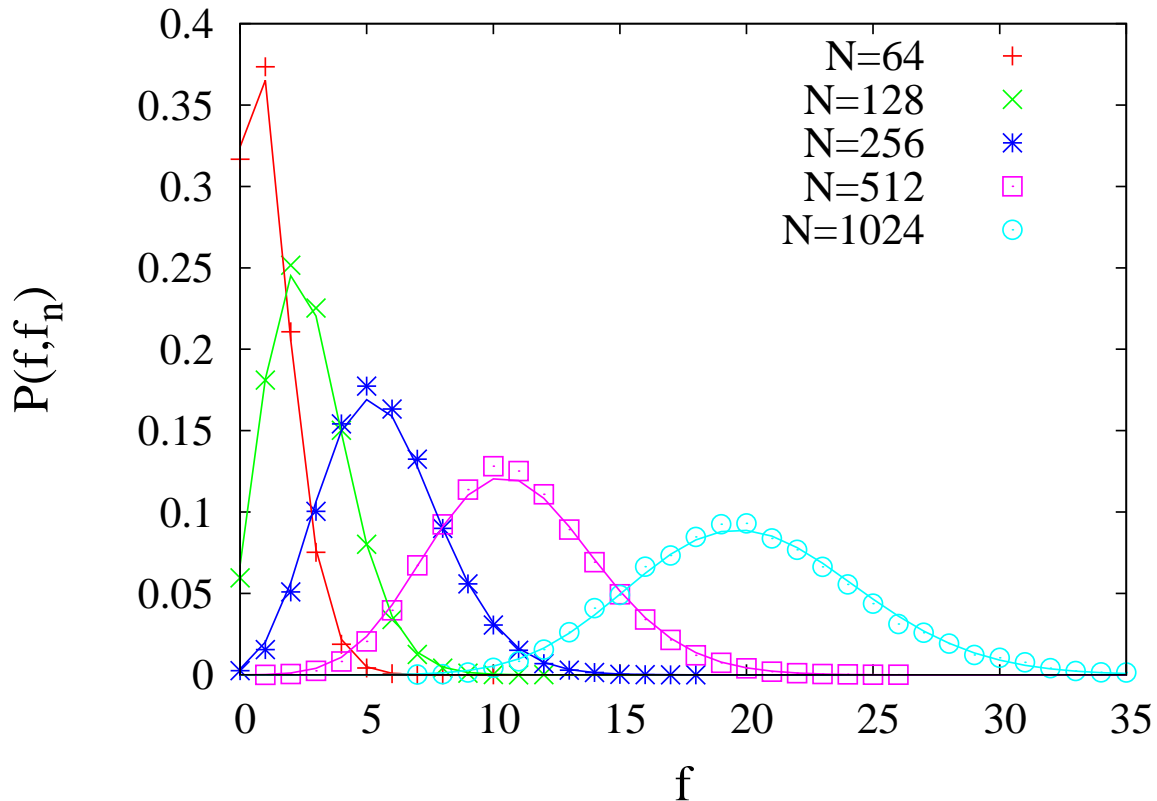


Figure 2. Distribution of the number of concatenations  $f$  per ring (data points) in mono-disperse solutions of interpenetrating rings at  $\phi = 0.5$ . The lines are computed using equation (3) and the average number of concatenations  $f_n$  as the only adjustable parameter.

area of the minimal surfaces of rings of same degree of polymerization at the same preparation conditions can be assumed because of the dominance of the boundary region of the area (see ref. [20]). Let us assume that concatenation is a random process that occurs with equal probability per polymer strand that passes through this rather constant area of the minimum surface. Under these conditions, the distribution of concatenated states is expected [21] to be described by a Poisson distribution

$$P(f, f_n) = \frac{f_n^f}{f!} e^{-f_n} \quad (3)$$

around the number average number of concatenations,  $f_n$ , per ring. Figure 2 shows an excellent agreement between equation (3) and the data of the computer simulations independent of the degree of polymerization  $N$  and the average number of concatenations  $f_n$ . The weight average functionality of the above Poisson distribution [22] is

$$f_w = f_n + 1 \quad (4)$$

and fits well to the simulation data as shown in Figure 3. Note that the cut-off for non-concatenation,  $P_{OO}$ , is only a weak correction at the gel point (of order 10%) and can be safely

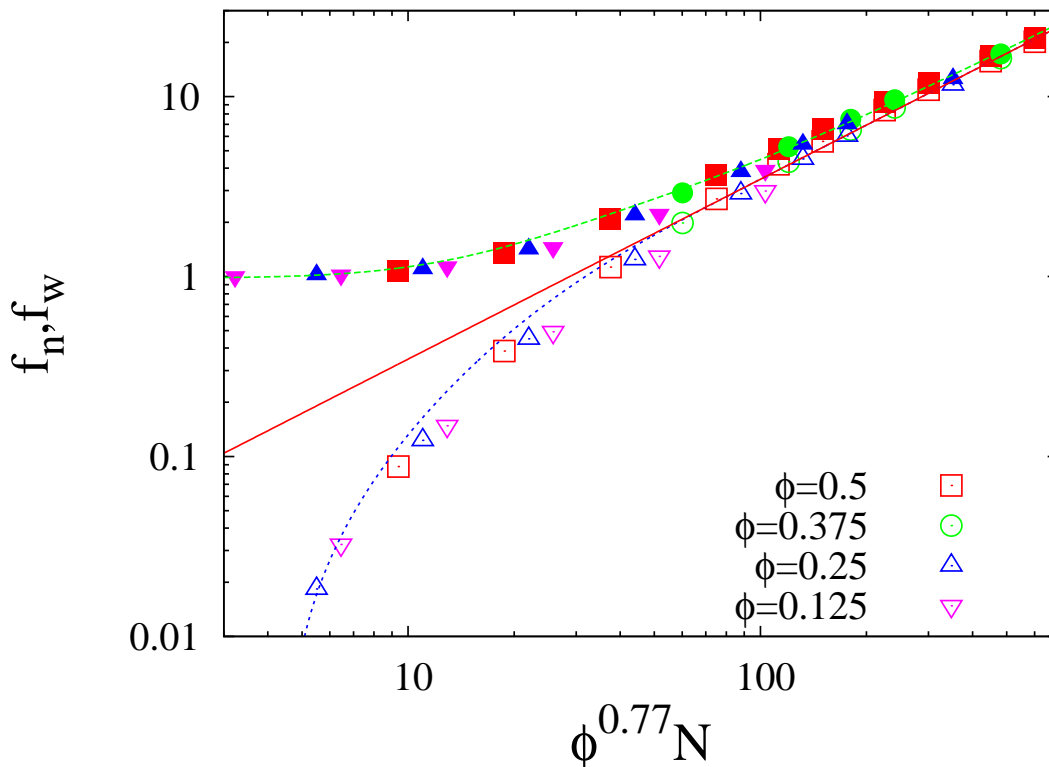


Figure 3. Number average  $f_n$  (hollow symbols) and weight average  $f_w$  (filled symbols) number of concatenations of cyclic polymers in mono-disperse solutions of cyclic polymers. The continuous line is a linear increase, the dotted line is equation (1), and the dashed green line is equation (4).

ignored for well developed gels.

The above estimate  $f_w = 2$  for the position of the gel point is tested by computing the size of the largest cluster of concatenated rings in the samples. The result is shown in Figure 4. According to the simulation data of networks close to the gel point (see also Figure 4), the gel point is located at a weight average functionality  $f_{w,c} = 2.12 \pm 0.03$ .

To estimate the the weight fractions of active material and gel, we use the approach of Miller and Macosko [23, 24] and apply it to a Poisson distributed set of functionalities with given average  $f_n$ . Let  $P_{out}$  denote the probability of finding a finite chain when “looking out” along one of the  $f$  connections (concatenations) of a ring. The functionality of the connected ring is selected randomly according to the weight fraction of connections to rings with  $f$  connections,

$$a_f = \frac{P(f, f_n) f}{\sum_f P(f, f_n) f} = \frac{f_n^{f-1}}{(f-1)!} e^{-f_n} = P(f-1, f_n). \quad (5)$$

Above we made use of  $\sum_f P(f, f_n) f = f_n$ . Note that the situation we analyze here is equivalent to full conversion  $p = 1$  in Refs. [23, 24] and thus, looking “out” or “into” a molecule from a

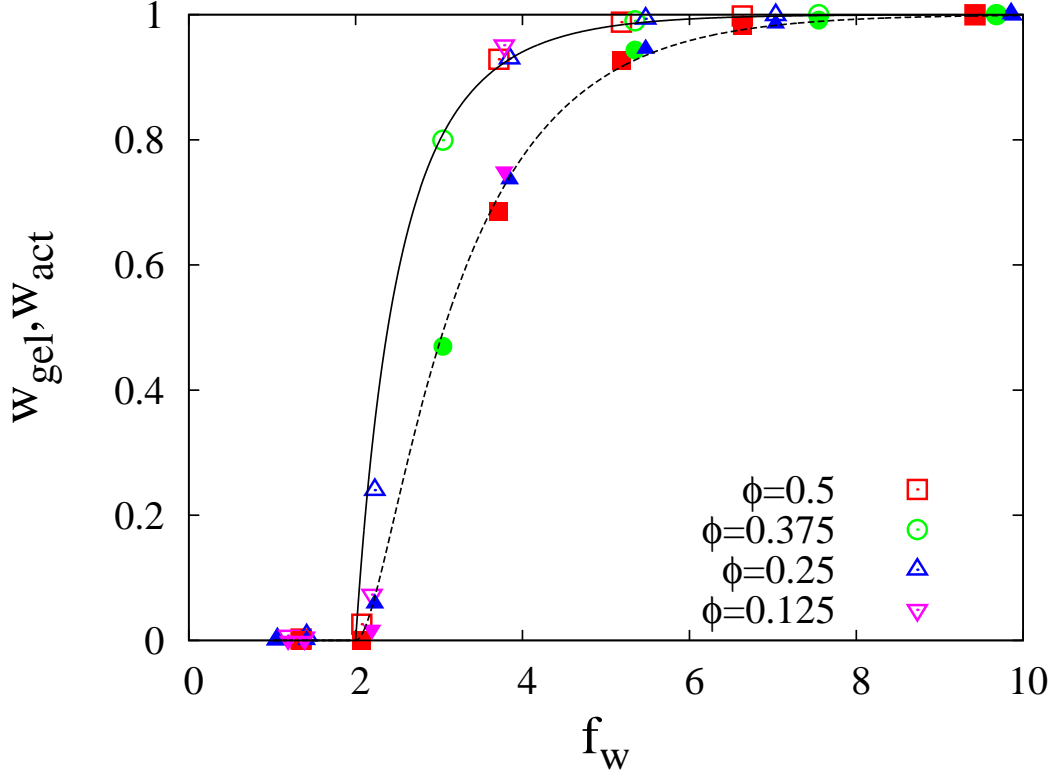


Figure 4. The weight fractions of the largest connected cluster of concatenated rings (hollow symbols) and the elastically active material (full symbols) as function of the weight average functionality of the rings. Continuous line is weight fraction of gel, equation (9), and dashed line is weight fraction of active material, equation (10).

given connection is equivalent:

$$P_{out} = P_{in} = \sum_f a_f P_{out}^{f-1}. \quad (6)$$

Thus, we need to solve numerically

$$\sum_f a_f P_{out}^{f-2} - 1 = 0 \quad (7)$$

for  $P_{out}$  as function of  $f_n$ , which is the only variable here. We seek a solution of this equation within the interval  $[0, 1[$ , if existing; otherwise  $P_{out} = 1$ . The weight fraction of sol,  $w_{sol}$ , and gel,  $w_{gel}$ , are computed by inserting this particular solution for  $P_{out}$  into the following equations:

$$w_{sol}(f_n) = \sum_f P(f, f_n) P_{out}^f \quad (8)$$

$$w_{gel}(f_n) = 1 - w_{sol} \quad (9)$$



The weight fraction of the active material,  $w_{act}$ , is the weight fraction of all rings in gel with at least two independent connections to the gel

$$w_{act}(f_n) = w_{gel}(f_n) - \sum_f P(f, f_n) f P_{out}^{f-1} (1 - P_{out}). \quad (10)$$

The above predictions are compared with simulation data in Figure (4). We observe good agreement with our mean field estimate for both weight fraction of gel and active material. Note that in contrast to conventional gelation the functionality of the molecules is not determined by chemistry; instead it results from the interpenetration and concatenation of overlapping rings. The external parameters  $N$  and  $\phi$  enter directly via  $f_n$  in the sol-gel transition and not in corrections for intra-molecular reactions as typical for chemically linked gels. Corrections to gelation (e.g. shift of gel point) are also expected to be universal here, since such corrections can only arise from multiple links between overlapping rings, that depend in the same manner from overlap between the molecules as concatenation. Note that the above analysis allows to determine  $f_w$  and thus,  $\gamma$  from experimental data in the region just above the gel point by measuring the weight fraction of solubles. Finally, we would like to point out that OGs with  $f_n \gtrsim 8$  can be considered essentially as defect free model systems, since  $w_{gel} > 0.999$  and  $w_{act} > 0.99$ . This ideal case of interpenetrating solutions is used in the following two sections below as reference to analyze DNA-Origami and progressive construction.

#### IV. DNA-ORIGAMI

To analyze the competition between the growth of linear chains and ring closure, we equilibrated melts of linear chains with rather small degrees of polymerization  $N = 16, 32,$  and  $64$  in order to achieve significant amounts of ring molecules upon randomly linking all chain ends. The total number of monomers in each sample was  $2^{20}$ . The linear chains were randomly assigned to be part of one of the  $B = 1, 2, 4, 8, 16, 32,$  or  $64$  batches of chains. Polymer volume fraction was kept constant at  $\phi = 0.5$  and all samples were simulated on a lattice of  $256^3$  lattice sites. A permanent bond is introduced whenever two previously unreacted chain ends of the same batch hit each other during the course of their motion at the smallest possible separation on the lattice. The extent of reaction at the end of the simulations was typically above 99% of the maximum possible extent of reaction. However, all samples were analyzed at conversion of  $p = 0.9568$ , which is the smallest maximum conversion that was achieved within all samples, in order to eliminate systematic effects caused by a variation of  $p$ . The number and weight fractions of linear chains and cyclic polymers of different size were analyzed at the end of the simulations.

Let us assume that at the beginning of the reaction, all chains are mono-disperse with a degree of polymerization  $N \gg 1$  such that ring formation is not restricted within individual chains. The overlap number

$$P \approx \phi R_g^3 / N \quad (11)$$

describes the number of chains in the pervaded volume of a polymer at the beginning of the reactions. Splitting the chains into  $B$  batches of chains that react selectively within the same batch reduces the overlap number to  $\approx \phi R_g^3 / (BN) = P/B$ . Pickett [5] expects that the weight fraction of rings among all polymer,  $w_O$ , can be described by a function of form

$$w_O \approx \frac{1}{1 + zP/B}, \quad (12)$$

whereby  $z$  is a numerical constant close to two reflecting the fact that only one opposite chain end is in the vicinity for ring formation, while each overlapping linear chain contributes two reactive groups. Our simulation data in the ‘‘dilute’’ regime  $B > P$  is well described by this prediction with  $z \approx 1.60 \pm 0.05$  as adjustable parameter, see Figure 5. However, the available data at  $P/B > 1$  seems to be a function of  $P/B$ , such that

$$w_O \approx y (P/B)^\alpha \quad (13)$$

with  $\alpha \approx -0.12 \pm 0.03$  and  $y \approx 0.36 \pm 0.02$ .

We searched literature for explanations of the regime  $P/B > 1$ , but neither a numerical test [25] of the compact exploration of space of the reactive chain ends [26] (resulting in a much larger  $\alpha$ ) nor an explicit computation of the self-dilution effect [27, 28] by using the mean field rate equations of the Appendix lead to convincing results (see Figure 5).

In addition to the above trends for the total weight fraction of cyclic polymers,  $w_O$ , we observe a qualitative change in the number fraction distributions  $n_i$  of linear chains and rings made of  $i$  precursor chains for the two regimes  $P/B > 1$  and  $P/B < 1$  as shown in Figure 6 and 7. The data below overlap,  $P/B < 1$  can be approximated by the set of differential equations given in the appendix. The effect of self-dilution is visible here by the depletion of shortest linear chains as compared to a most probable distribution (linear decay on semi-log plot). The decay of the number fraction of rings at small  $i$  can be approximated alternatively by a power law with an exponent near  $-3/2$  with an exponential cut-off similar to the distribution of the linear chains. In contrast to this, both distributions apparently become two most probable distributions with different effective conversions  $p$  in the regime  $P/B > 1$  in a first order approximation, see Figure 7. Here, the effective  $p$  to describe the distributions of the rings is always smaller as the one of the linear chains, which is close to equation (38) of the Appendix. Note that in both cases an

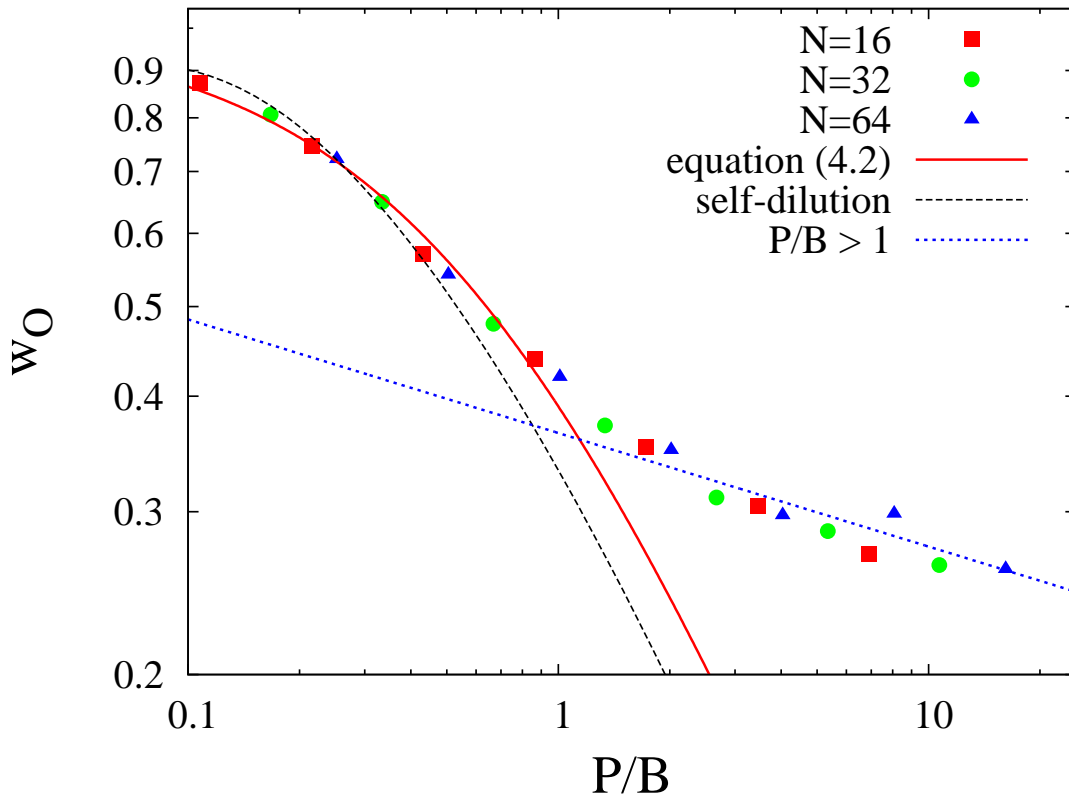


Figure 5. Weight fraction of cyclic polymers as function of the number of batches  $B$  rescaled to overlap concentration. The “self-dilution” estimate was computed for  $p = 0.9568$  and fit to the data for with  $w_O > 1/2$ , while the effect of  $p < 1$  was ignored for equation (12). The dotted line is a power law approximation for the tail at large  $P/B$  as discussed in the text.

efficient formation of concatenated rings is only possible, if the degree of polymerization of the precursor linear chains is already above the cut-off for non-concatenation.

Let us now discuss the gel point condition and network structure for DNA origami in both limits  $P/B < 1$  and  $P/B > 1$  based upon the available data. For simplicity, we assume, that the precursor chains have a higher degree of polymerization as the cut-off degree of polymerization for concatenation  $N > N_{OO}$ . This allows us to use the weight fraction of rings  $w_O$  as correction for the average number of concatenations and to drop the non-concatenation correction in equation (1).

In the limit  $P/B < 1$ , the number fraction distribution of rings is dominated by the strong decay at small  $i$  such that we can keep in first approximation  $f_w \approx f_n + 1$ , which simplifies the gel point condition to

$$\gamma\phi^{\nu(3\nu-1)}Nw_O \approx f_n \approx 1. \quad (14)$$

Under these conditions, all results of the previous section can be kept as first order approximation, after the average number of concatenations is corrected by a factor  $w_O$  as in the above

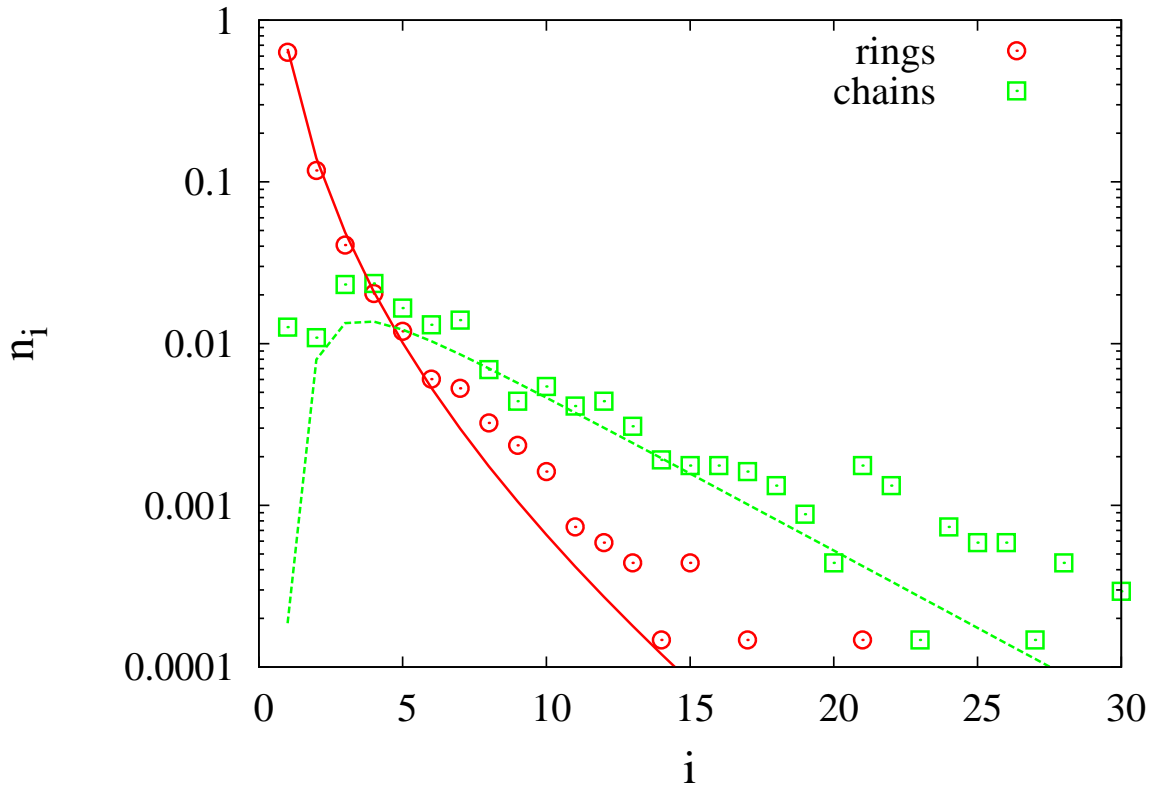


Figure 6. Typical number fraction distribution  $n_i$  of linear chains and cyclic polymers made of  $i$  precursor chains at  $P/B < 1$ . Data taken at  $p = 0.9568$  of a sample with  $N = 64$  and  $B = 32$ . Lines are computed using the differential equations described in the Appendix.

equation. The number of batches  $B$  necessary to pass through the gel point is here

$$B \approx \frac{zN^{1/2}}{\gamma\phi^{\nu(3\nu-1)}N - 1} \quad (15)$$

because of  $P \approx N^{1/2}$ . Since  $P/B < 1$ , there is  $B \gtrsim N^{1/2}$ , which yields that the above criterion holds for  $N\phi^{\nu(3\nu-1)} \lesssim (z+1)/\gamma$ . All samples with larger  $N\phi^{\nu(3\nu-1)}$  are gelled, if  $B > P$ .

Note that the above two equations can be used to map the DNA Origami in the regime  $P/B < 1$  in first approximation back onto the ideal OG case. For instance, considering our results for the ideal OGs we conclude that almost defect free model networks (after removal of linear chains) with a weight fraction of  $w_{net} \approx w_O$  are obtained for  $P/B < 1$ , if  $f_n \gtrsim 8$ .

In the limit  $P/B > 1$ , the number fraction distribution of rings is roughly given by a most probable weight distribution, see Figure 7. Because of the narrowly distributed functionalities for a given  $N$ , equation (3), the relation between number and weight average functionality is dominated by the broader distribution of the molecular weights. Thus,  $f_w \approx 2f_n$ . Thus, the gel point condition is the same as in equation (14) by coincidence. The weak dependence of  $w_O$  on  $P/B$  for  $P/B > 1$  shows that a variation of the number of batches for reaction is not

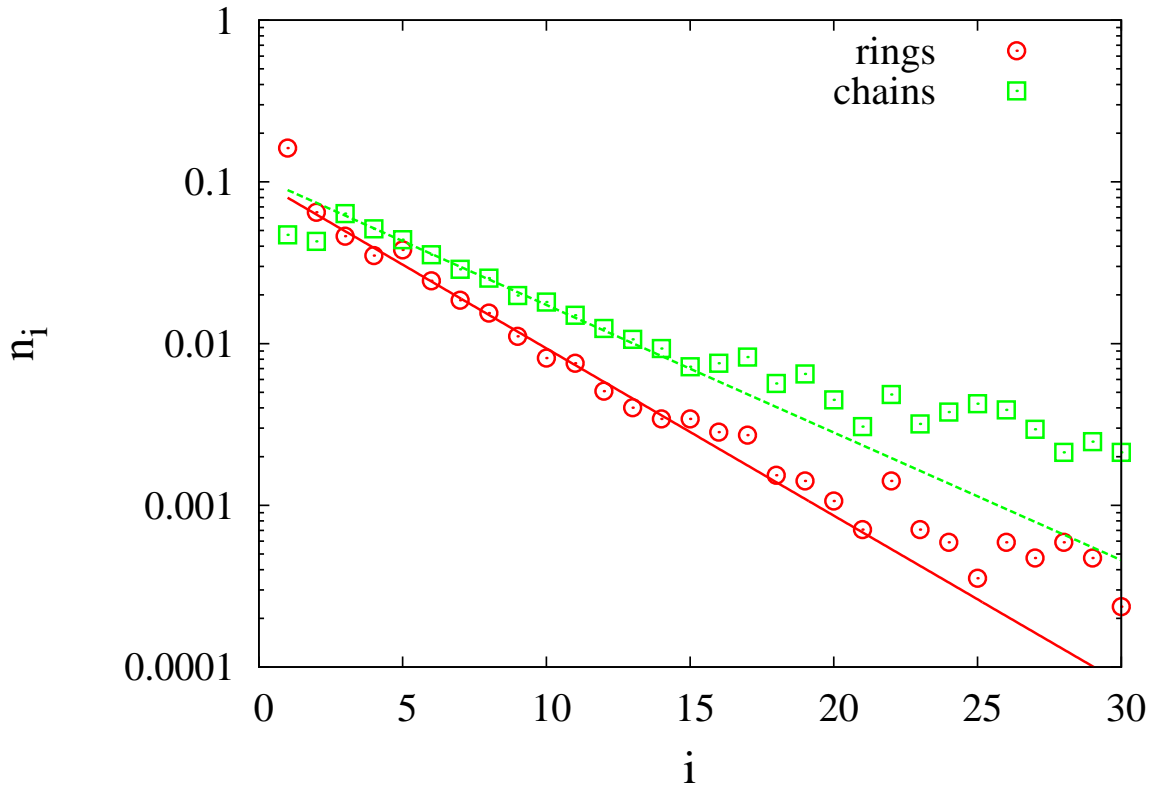


Figure 7. Typical number fraction distribution  $n_i$  of linear chains and cyclic polymers at  $P/B > 1$ . Data taken at  $p = 0.9568$  of a sample with  $N = 16$  and  $B = 1$ . Lines are fits to functions  $ap^{i-1}(1-p)$  with variables  $a$  and  $p$ .

very effective unless one reaches the opposite regime  $P/B < 1$ . On the other hand, since the average functionality of the rings grows  $\propto \gamma\phi^{\nu(3\nu-1)}N^{1-\alpha/2}$  for constant  $B$ , the probably most efficient strategy in this limit  $P/B > 1$  is simply to choose a precursor degree of polymerization  $N \gg N_{OO}$  such that  $f_n > 1$  despite the low  $w_O$ . However, this yields low network weight fractions  $w_{net} < w_O \ll 1$  and a high fraction of long linear chains  $1 - w_O$  needs to be extracted. As a result, one might obtain a largely de-swollen Olympic network.

We have to comment here, that the observed power law for  $w_O$  as function of  $B/P$  must not necessarily extend to ratios of  $P/B$  much larger than the ones obtained in our study - as it would be necessary to achieve gelation. The worst case scenario is here  $w_O \propto (P/B)^{-1}$ , which still leads at a constant  $B$  and  $\phi$  to a growing functionality of the rings,  $f_n \propto N^{1/2}$ , if  $N$  remains below an  $N^*$  above which any pair of overlapping rings is concatenated (see Ref. [11] for details). For  $N > N^*$  on the other hand,  $f_n$  becomes constant in this worst case scenario and increasing  $N$  beyond  $N^*$  will not cause the formation of an OG. However, for the worst case scenario  $w_O \propto (P/B)^{-1}$ , a variation of  $B$  is very effective, since  $f_n \propto B$  for both regimes  $N < N^*$  and  $N > N^*$ .

## V. PROGRESSIVE CONSTRUCTION

The results of the two previous sections can be applied to discuss the progressive construction methods for OGs. The original approach of Ref [4] is devoted to a mixture of long and short polymers that are both below the entanglement length in order to avoid complications by the compression of the long cyclic polymers. This requires that the concatenation degree of polymerization  $N_{OO}$  is clearly below the entanglement degree of polymerization  $N_e$ . In our previous work [11, 13], we rather find the opposite:  $N_{OO} \gtrsim N_e$ . Even ideal mono-disperse samples (see section III) do not form OGs for  $N < N_e \lesssim N_{OO}$ . Therefore, we develop an alternative approach for progressive construction at  $N > N_{OO}$  using the same strategy as proposed in Ref. [4]: we use short linear strands to link long non-concatenated rings that were concentrated above overlap concentration.

Let us use  $L$  and  $S$  to denote the degrees of polymerization of the long and short molecules respectively. Since the Kuhn molecular weight of the simulation model is close to one monomer, we drop all coefficients related to converting monomers to Kuhn monomers. Next,  $w_L$  and  $w_S$  denote the weight fractions of long and short rings among all polymer, while  $w_{lin}$  is the weight fraction of linear chains that is obtained as by-product of the linking reactions. Thus,  $w_L + w_S + w_{lin} = 1$ . Finally,  $\phi$  is the weight fraction of polymers,  $b$  the root mean square length of a segment and the monomeric volume  $v_0$  is  $\approx b^3$ .

First, let us consider the case  $w_S \ll w_L \approx 1$  so that conformational changes upon the addition of short polymers can be ignored in first approximation. Furthermore, we add short chains well below their overlap volume fraction such that  $w_S > w_{lin}$  and the cyclic chains produced by the  $S$ -mers consist predominantly of only one  $S$ -mer. Since the  $S$ -mers are dilute, we assume that  $S$ -mers entrap in first approximation only  $L$ -mers [29]. Thus,

$$f_{n,S} \approx \gamma \phi^{\nu/(3\nu-1)} S (w_L + w_S) \approx \gamma \phi^{\nu/(3\nu-1)} S. \quad (16)$$

These concatenations are distributed among all  $L$ -mers, for which we obtain a concatenation density that is reduced by a factor of  $w_S/w_L$ . This lower concatenation density determines the average number of concatenations of the long chains

$$f_{n,L} \approx \frac{w_S}{w_L} \gamma \phi^{\nu/(3\nu-1)} L. \quad (17)$$

In both cases, we expect that the number of concatenations are Poisson distributed [30]. For concatenations only between long and short rings we can map the problem to co-polymerizations of molecules with distributed functionalities that are discussed in Ref. [24]. Then, the gel point

condition can be written as

$$(f_{w,S} - 1)(f_{w,L} - 1) = f_{n,S}f_{n,L} \approx \frac{w_S L}{w_L S} f_{n,S}^2 = 1. \quad (18)$$

Thus,  $w_L \gg w_S$  requires that  $Lf_{n,S}^2/S \gg 1$ , which is best obtained for  $f_{n,S} \gtrsim 1$  in order to avoid gigantically long polymers  $L$ , since for very small  $f_{n,S}$  the exponential cut-off for concatenation [11] would lead to a square exponential growth of  $L$ . In contrast to this result,  $f < 1$  has been suggested in Ref. [4] for the small rings to create OGs. Another interesting point of equation (18) is that it allows to determine  $\gamma$  experimentally, if the polydispersity of the rings made by  $S$ -mers is low, since then, all parameters of this equation except of  $f_{n,S}^2$  and thus,  $\gamma$  are known.

Similar to section III, the final goal is to achieve OGs with a well developed network structure such that essentially all  $L$ -mers are active. Since linking of long chains should happen by a volume fraction of short chains below their overlap volume fraction (note that  $S$ -mers are larger than blob size at  $f_{n,S} > 1$ ), we require

$$w_S \phi < \phi_S^* \approx \frac{b^3 S}{(bS^{1/2} \phi^{-(\nu-1/2)/(3\nu-1)})^3}, \quad (19)$$

which is

$$w_S \lesssim S^{-1/2} \phi^{-(6\nu-5/2)/(3\nu-1)} \quad (20)$$

as upper limit for  $w_S$ . Let us use this upper limit as bound for the maximum weight fraction to be added to obtain a “well developed” network. Using the results of the ideal OGs of section III as reference, let us adopt the following criteria  $f_{n,L}f_{n,S} \geq 8$  and  $f_{n,S} \geq 1$  to ensure that essentially all large rings are incorporated into the gel. Thus, we require

$$\frac{w_S L}{w_L S} f_{n,S}^2 \geq 8 \quad (21)$$

at the end of the reactions. A weight fraction  $w_S$  that fulfills equation (20) and (21) can be found, if

$$L \geq 8w_L S^{-1/2} \gamma^{-2} \phi^{-(5/2-4\nu)/(3\nu-1)}, \quad (22)$$

which requires an enormous  $L \gtrsim 900$  for our simulations to start with, because here  $\gamma^{-1} \approx 30$  and  $S \geq 50$  for  $f_{n,S} \geq 1$  (at  $\phi = 0.5$ ). This result shows that the construction of well developed OGs is possible within a single concatenation step, given that sufficiently long chains  $L$  are available to be linked.

More details about network structure can be obtained numerically using the approach of Miller and Macosko [23, 24] applied to co-polymerization similar to our discussion in section III.

One interesting point is here, that the weight fraction of sol could be used for an alternative determination of  $f_{n,S}$  and thus  $\gamma$  if  $f_{n,S}$  is sufficiently large such that the exponential cut-off for  $f_{n,S}$  could be ignored. This is because  $f_{n,S}$  is Poisson distributed and a fraction of  $e^{-f_{n,S}}$  of the short chains will not entrap any polymer. Thus, well beyond the gel point,  $f_{n,S}f_{n,L} \gg 1$ , the weight fraction of sol will be dominated by non-concatenated short chains and linear strands,  $w_{sol} \approx w_{lin} + w_S e^{-f_{n,S}}$ , which may be used to estimate  $f_{n,S}$ , if  $w_{lin}$  is sufficiently small or linear chains can be separated from cyclic polymers.

A combination of progressive construction and DNA-Origami would allow to increase the lower boundary for the weight fraction of the short polymers,  $w_S$ , in equation (20) by a factor equal to the number of batches,  $B$ , such that the required chain length  $L$  is reduced to  $L/B$ . However, a too large  $B$  will break the assumption [31]  $w_S \ll w_L$  which is for  $B = 1$  essentially always satisfied because of the low value of  $\gamma$ . Instead, if a large  $B$  is available, it could be used to minimize  $w_{lin}$  instead in order to remove effects of poly-disperse rings made of  $S$ -mers and to reduce the weight fraction of sol.

On the other hand, the combination of DNA-Origami and progressive construction can be used to reduce the weight fraction of sol for a given possible maximum number of batches  $B$  as compared to pure DNA-Origami. As trade off one obtains a sample that consists of partially compressed long chains concatenated with short chains that are at equilibrium at cross-linking conditions, which is the general complication of creating OGs by progressive construction. Indeed, for progressively constructed gels one has to expect an even more unusual swelling behavior as found recently for ideal OGs [3], since beyond dis-interpenetration of rings, the long rings gain extra conformations by reducing their compression.

## VI. SUMMARY

In the present paper we have discussed analytically and numerically the formation and structure of Olympic gels (OGs) and tested our predictions by simulation data. We focused on three different model cases: ideal OGs, DNA-Origami, and progressive construction. For ideal OGs we demonstrate that the distribution of the number of concatenations is well approximated by a Poisson distribution. This Poisson distribution can be used to predict numerically structural features of the gels, such as the gel point, the weight fraction of gel, or the weight fraction of elastically active rings. These predictions are well supported by simulation data. While the construction of ideal OGs was not considered explicitly in previous work, we found for the other two cases clear differences to previous works [4, 5].

Below overlap concentration of the linear chains used for DNA-Origami, the model of Pickett



[5] is well suited to describe the weight fraction of rings. Above overlap, we find a much smaller decay of the weight fraction of rings as function of the overlap number  $P$  and the number of batches  $B$  with selectively binding ends that is  $\propto (P/B)^\alpha$  with an  $\alpha \approx -0.12 \pm 0.03$ . A more detailed mean field analysis taking into account the competition between ring formation and growth of linear chains does not lead to an improved description of the simulation data. However, following the results of the mean field model one can conclude that by far the most efficient way to achieve a large weight fraction of rings is to choose a low overlap  $P/B$  of the linear chains at the onset of the reaction. Since the weight fraction of rings is dominated by the smallest rings, possible steric cut-offs for ring formation and concatenation seriously affect the formation of rings that can concatenate.

Progressive construction can be used indeed, to obtain OGs. However, the conditions necessary for gelation are rather opposite to the ones proposed originally by [4]: instead of using very short strands with a number average number of concatenations  $f_n < 1$ , we suggest to use  $f_n > 1$ , since otherwise, the required minimum degree of polymerization of the long rings,  $L$ , will grow square exponential when further reducing  $f_n$ . The Poisson distribution for the number of concatenations allows again to derive a rather simple condition for gelation. However, the low numerical constant  $\gamma$  for concatenation leads to still very large  $L$  to obtain well developed OGs, if the weight fraction of the short polymers is low in order to not disturb the conformations of the long chains.

In general, DNA-Origami can be combined with progressive construction. This allows to either use a smaller number of batches as compared to DNA-Origami, or a smaller  $L$  could be used in progressive construction, which may simplify the construction of OGs.

## VII. ACKNOWLEDGEMENT

The authors acknowledge a generous grant of computing time at the ZIH Dresden for the project BiBPoDiA. Financial support was given by the DFG grants LA 2735/2-1 and SO 277/7-1.

- 
- [1] P. G. de Gennes, “Scaling Concepts In Polymer Physics”, Cornell University Press, New York, NY, USA (1991).
  - [2] T. A. Vilgis and M. Otto, *Phys. Rev. E* **56**, R1314 (1997).
  - [3] M. Lang, J. Fischer, M. Werner, and J.-U. Sommer, *Phys. Rev. Lett.* **112**, 238001 (2014).
  - [4] E. Raphael, C. Gay, and P. G. de Gennes, *J. Stat. Phys.* **89**, 111 (1997).
  - [5] G. T. Pickett, *Europhys. Lett.* **76**, 616 (2006).

- [6] I. Carmesin and K. Kremer, *Macromolecules* **21**, 2819 (1988).
- [7] K. Binder and H. Deutsch, *J. Chem. Phys.* **94**, 2294 (1991).
- [8] J. P. Wittmer, P. Beckrich, H. Meyer, A. Cavallo, A. Johner, and J. Baschnagel, *Phys. Rev. E* **76**, 11803 (2007).
- [9] M. Lang, M. Rubinstein, and J.-U. Sommer, *ACS Macro Letters* **4**, 177 (2015).
- [10] W. Paul, K. Binder, D. W. Heermann, and K. Kremer, *J. Phys. II France* **1**, 37 (1991).
- [11] M. Lang, J. Fischer, and J.-U. Sommer, *Macromolecules* **45**, 7642 (2012).
- [12] M. Lang and J.-U. Sommer, *Phys. Rev. Lett.* **104**, 177801 (2010).
- [13] M. Lang, *Macromolecules* **46**, 9782 (2013).
- [14] M. Lang, W. Michalke, and S. Kreitmeier, *J. Comp. Phys.* **185**, 549 (2003).
- [15] G. Gouesbet, S. Meunier-Guttin-Cluzel, and C. Letellier, *Applied Mathematics and Computation* **105**, 271 (1999).
- [16] P. Freyd, D. Yetter, J. Hoste, W. Lickorish, K. Millet, and A. Ocneanu, *Bull. Am. Soc.* **12**, 239 (1985).
- [17] W. Michalke, M. Lang, S. Kreitmeier, and D. Göritz, *Phys. Rev. E* **64**, 012801 (2001).
- [18] M. Tanaka, K. Iwata, and N. Kuzuu, *Comp. Theo. Pol. Sci.* **10**, 299 (2000).
- [19] P. J. Flory, “Principles Of Polymer Chemistry”, Cornell University Press, Cornell, NY, USA (1953).
- [20] M. Lang, *Macromolecules* **46**, 1158 (2013).
- [21] The Poisson distribution is the mathematical approximation of independent random events which occur at low average rate. By using this approximation, we thus, implicitly ignore additional conditions to the underlying random process as may result from packing conditions and neglect possible correlations among concatenations: For instance, each concatenation blocks a certain volume near the minimal surface for other cyclic molecules and thus, a weak anti-correlation (repulsion) among concatenating molecules is to be expected, which should lead to a narrowing of the distributions. Since the deviations between data and Poisson distribution in Figure 2 are rather small, these additional effects are either ignorable or compensated by the neglect of the minimal area distribution of the rings mentioned previously.
- [22] L. H. Peebles, “Molecular Weight Distributions in Polymers”, Wiley, New York, USA (1971).
- [23] D. Miller and C. Macosko, *Macromolecules* **9**, 206 (1976).
- [24] C. Macosko and D. Miller, *Macromolecules* **9**, 199 (1976).
- [25] Y.-K. Leung and B. Eichinger, *J. Chem. Phys.* **80**, 3885 (1984).
- [26] P. de Gennes, *J. Chem. Phys.* **76**, 3316 (1982).
- [27] H. R. Kricheldorf, S. Böhme, and G. Schwarz, *Macromolecules* **34**, 8879 (2001).
- [28] H. R. Kricheldorf and G. Schwarz, *Macromol. Rapid Commun.* **24**, 359 (2003).
- [29] Actually, there is an entropic bias towards penetration of long chains, if the long chains are compressed.
- [30] Here, concatenations of  $L$  rings are caused only by  $S$  rings, which are dilute in the melt of  $L$  rings. Thus, the positions of the  $S$  rings are not correlated and the rate of concatenation for line elements of the  $L$  rings are low. Therefore, the  $L$  rings must show a Poisson distribution of concatenations.

The concatenation distribution of  $S$  rings, on the other hand, can be mapped onto the monodisperse ideal Olympic gel case, since the number of strands of large  $L$  rings that overlap with the  $S$  ring is of order  $S^{1/2}$ . However, packing constraints might be somewhat relaxed here, which could lead to a slightly broadened distribution in the number of concatenations as compared to the monodisperse case.

- [31] And thus, swell the long chains and cause a significant fractions of S-mer concatenations by S-mers. This may complicate a theoretical description of these samples, but it will clearly allow to obtain well developed OGs at a lower  $L$ .

## VIII. APPENDIX:

### A. Mean field approximation of ring-chain competition

The competition between the growth of linear chains and ring formation can be analyzed numerically in a mean-field framework by an adequate set of differential equations. We consider first the linear condensation of short  $N$ -mer chains (monomers “A”) without ring formation. Let  $n_i(p)$  denote the number fraction of  $iN$ -mers at conversion  $p$ . At the absence of ring formation, one obtains for irreversible linear condensation reactions of monomers A



a most probable weight distribution with the well known polymer number fraction distribution

$$n_i(p) = p^{i-1}(1-p) \quad (24)$$

and an average degree of polymerization that is here

$$N_n = N \frac{1}{1-p}. \quad (25)$$

A numerical solution of this problem can be computed using the following set of differential equations: The number fraction  $di^-(p)$  of  $i$ -mers that react within a integration interval  $dp$  is

$$di^-(p) = n_i(p)dp, \quad (26)$$

while the fraction  $di^+(p)$  of  $i$ -mers formed during the integration interval is given by

$$di^+(p) = \sum_{k=1}^{i-1} n_k(p)n_{i-k}(p)dp. \quad (27)$$

Since the distribution  $n_i(p)$  is normalized to one, the change in conversion equals  $dp$ . With initial conditions  $n_1(0) = 1$  and  $n_i = 0$  for  $i > 1$  we obtain numerically equation (25), by computing

$$n_i(p+dp) = n_i(p) + di^+(p) - di^-(p) \quad (28)$$

in infinitesimal integration intervals  $dp$ . The analytical solution, equation (25), can be used to check the accuracy of the numerical solution.

Ring formation is implemented using the same assumptions (Gaussian statistics for all  $iN$ -mers, mean field approximation) as in section IV. The average concentration of the reactive groups  $c(p)$  is proportional to the initial concentration  $c_0$  of reactive groups and decays with conversion

$$c(p) = c_0(1 - p). \quad (29)$$

Gaussian statistics for all precursor chains and combined linear chains of  $i$  sections with  $N$  monomers leads to concentrations

$$c_i \approx c_1 i^{-3/2} \quad (30)$$

of the first end of an  $iN$ -mer near its second end. Here  $c_1 \approx 1/(2P)$  is the corresponding concentration for one chain of  $N$  monomers. Assuming equal reactivity, all reaction rates are proportional to the concentrations of the reactive species only. Thus, we can equate for the rate to form a ring polymer of  $iN$  monomers,  $dC_i^+$ , that

$$\frac{dr_i^+(p)}{di^-(p)} = \frac{c_i}{c_0(1 - p)}. \quad (31)$$

These additional reactions that convert linear chains of  $iN$  monomers into cycles disturb the most probable distribution of the linear species. Nevertheless, the total number fraction of all species is still normalized,

$$\sum_i n_i(p) + \sum_i r_i(p) = 1, \quad (32)$$

whereby only the number fraction of linear chains,

$$n_{lin}(p) = \sum_i n_i(p), \quad (33)$$

is available for further reactions. Note that in the above equations  $d_i^+(p)$  is  $\propto n_{lin}^2(p)$ , while  $d_i^-(p)$  and  $dr_i^+(p)$  are proportional to  $n_{lin}(p)$ . Therefore, we have to modify equation (27) to

$$di^+(p) = \sum_{k=1}^{i-1} n_k(p)n_{i-k}(p)dp/n_{lin}(p), \quad (34)$$

if there is ring formation in order to maintain normalization of the distributions. The number fractions of rings and linear chains are obtained by computing

$$r_i(p + dp') = r_i(p) + dr_i^+(p) \quad (35)$$

$$n_i(p + dp') = n_i(p) + di^+(p) - di^-(p) - dr_i^+(p). \quad (36)$$

Note that the effective infinitesimal conversion  $dp'$  is affected by ring forming reactions leading to

$$dp' = \sum_i (di^-(p) + dr_i^+(p)). \quad (37)$$

Ring formation also modifies the conversion of the linear species, since  $p \equiv 1$  for all rings. Let  $w_O(p)$  denote the weight fraction of rings at conversion  $p$ . The conversion among the linear chains,  $p_{lin}$ , is thus given by

$$p_{lin} = \frac{p - w_O(p)}{1 - w_O(p)}. \quad (38)$$

This relation can be used to compute  $p$  directly from the average degree of polymerization of the linear chains,  $N_n$ , by inserting  $p_{lin}$  instead of  $p$  into equation (25) for the linear species.